

Mapping the Backbone Dihedral Free-Energy Surfaces in Small Peptides in Solution Using Adiabatic Free-Energy Dynamics

Lula Rosso,^{†,‡} Jerry B. Abrams,[‡] and Mark E. Tuckerman^{*,§}

Departments of Chemistry and of Chemistry and Courant Institute of Mathematical Sciences,
New York University, New York, New York 10003

Received: October 8, 2004; In Final Form: December 22, 2004

Ramachandran surfaces for the alanine di- and tripeptides in gas phase and solution are mapped out using the recently introduced adiabatic free-energy dynamics (AFED) approach introduced by Rosso et al. (*J. Chem. Phys.* **2002**, *116*, 4389) as applied to the CHARMM22 force field. It is shown that complete surfaces can be mapped out with an order of magnitude of greater efficiency with the AFED approach than they can using the popular umbrella sampling method. In the alanine dipeptide, it is found, in agreement with numerous other studies using the CHARMM22 force field, that the lowest free-energy structure is the extended β conformation, $(\phi, \psi) = (-81, 81)$, while in solution, the extended β , $(\phi, \psi) = (-81, 153)$ and right-handed α -helical, $(\phi, \psi) = (-81, 63)$ conformations are nearly isoenergetic. In solution, a secondary minimum at $(\phi, \psi) = (63, -81)$, corresponding to a C_7^{ax} conformation, occurs approximately 2.3 kcal/mol above the global free-energy minimum. The alanine tripeptide, a system that has received considerably less attention in the literature, is found to exhibit a similar structure to the alanine dipeptide with the extended β conformation being the free-energy minimum in the gas phase and the β and right-handed α -helical conformations being isoenergetic in solution. These studies indicate that the AFED method can be a powerful tool for studying multidimensional free-energy surfaces in complex systems.

1. Introduction

The conformational equilibria of small peptides give important insights into secondary structural motifs that occur in the folds of larger proteins and peptides.¹ As new experimental techniques emerge that are capable of probing key aspects of the structure and dynamics of small peptides,^{2–7} it is critical to develop theoretical methods capable of aiding in the interpretation of such experiments or suggesting directions for further experimentation. One of the most widely used methods for studying such conformational equilibria is classical molecular dynamics (MD), which has emerged as a powerful tool for elucidating both structural and dynamical properties. Despite its widespread use, however, MD suffers from a severe lack of ergodicity when applied to systems described by rough energy landscapes, i.e., potential surfaces on which important minima are separated by high-energy barriers. This lack of ergodicity leads to a dramatic loss of efficiency. That is, in such cases, MD is unable, on time scales routinely accessed with modern day computers, to obtain a statistically meaningful sampling of the full conformational space, from which population distributions and free-energy surfaces are obtained. Indeed, it still remains one of the computational grand challenge problems to develop techniques capable of enhancing sampling and extending the accessible time scales in MD calculations.

At present, only a handful of techniques exist for probing multidimensional free-energy surfaces via MD or Monte Carlo simulations.^{8–18} Recently, we introduced new methodol-

ogy^{16,17,19} for enhancing conformational sampling in MD calculations. The underlying mathematical framework of the approach is the use of variable transformations that isolate a set of coordinates important in the sampling problem. These coordinates are then either subject to an adiabatic separation from the remaining degrees of freedom, allowing the free-energy hypersurface to be generated directly from the adiabatic probability distribution function^{16,19} or used in further variable transformations that warp the conformational space so as to expand attractive basins and remove barrier regions.¹⁷ Both methods have been shown to enhance conformational sampling in linear chains such as alkanes. Moreover, because points along the subspace of the chosen coordinates are visited frequently over the course of the trajectory, hysteresis problems, which plague umbrella sampling²⁰ and thermodynamic integration methods,^{21,22} are largely avoided. Here, we present the first application of the adiabatic dynamics methodology to an all-atom model of small peptides. In the present study, it will be shown how to use the adiabatic free-energy dynamics (AFED) method of Rosso et al.^{16,19} to obtain (ϕ, ψ) free-energy surfaces and Ramachandran contour maps for small polypeptides, here, the alanine di- and tripeptides in both gas phase and in an explicit solvent. Comparisons of accuracy and efficiency will be made with the popular umbrella sampling method.²⁰

The alanine dipeptide is one of the most widely studied small peptide systems, and consequently, its conformational space has been analyzed in detail for a variety of different force fields (see refs 23–28 as examples of such studies). Thus, the alanine dipeptide serves as an important system against which to benchmark the AFED method. The alanine tripeptide, on the other hand, has received considerably less attention in the literature,^{7,25,29–32} and hence, its conformational space is not as well-characterized. The alanine tripeptide, which contains three

* To whom correspondence should be addressed. Telephone: 212-998-8471. Fax: 212-260-7905. E-mail: mark.tuckerman@nyu.edu.

[†] Present address: Department of Chemistry, Imperial College, Exhibition Road, London SW72AY, U.K.

[‡] Department of Chemistry.

[§] Department of Chemistry and Courant Institute of Mathematical Sciences.

peptide bonds and two sets of dihedral (ϕ , ψ) angles, is the smallest peptide system that contains more than a single (ϕ , ψ) pair. It, therefore, offers the opportunity to investigate correlations that might exist between the two dihedral angle pairs in a simple peptide system and characterize the influence of solvent on the conformational equilibria.

The organization of the paper is as follows: A brief review of the AFED technique is presented in section 2, and details of the present simulations are given. In sections 3 and 4, the efficiency of the AFED method is compared with the widely used sampling method, the umbrella sampling approach,²⁰ on the alanine di- and tripeptide systems both in the gas phase and in solution. It is shown that AFED allows two-dimensional surfaces to be generated nearly an order of magnitude more efficiently than umbrella sampling. In section 3, results for the alanine dipeptide system are compared with other studies in the literature, and new results for the alanine tripeptide are presented in section 4. Conclusions and further directions are given in section 5.

2. Methodology and Simulation Details

The AFED approach¹⁶ employs a variable transformation in the canonical partition function to isolate a reactive subspace, and then imposes an adiabatic separation on this subspace to generate an adiabatic probability distribution function from which the free-energy surface can be obtained directly. Because AFED is based on a variable transformation, it differs fundamentally from other adiabatic schemes.¹⁸ The adiabatic separation causes the degrees of freedom orthogonal to the reactive degrees of freedom to sample large portions of their conformational space as the reactive coordinates slowly evolve. The reactive coordinates, on the other hand, sample a hypersurface that is more characteristic of the free-energy hypersurface than of the bare potential surface.

Consider a classical N -particle system with masses m_1, \dots, m_N , coordinates $\{\mathbf{r}_1, \dots, \mathbf{r}_N\} \equiv \mathbf{r}$, and momenta $\{\mathbf{p}_1, \dots, \mathbf{p}_N\} \equiv \mathbf{p}$ in a containing volume V at temperature T . The canonical partition function is given by

$$Q(N,V,T) = \frac{1}{N!h^{3N}} \int d^N \mathbf{p} \int_{D(V)} d^N \mathbf{r} \times \exp \left\{ -\beta \left[\sum_{i=1}^N \frac{\mathbf{p}_i^2}{2m_i} + U(\mathbf{r}_1, \dots, \mathbf{r}_N) \right] \right\} \quad (1)$$

where h is Planck's constant, $\beta = 1/k_B T$, $D(V)$ is the spatial domain defined by the containing volume, and $U(\mathbf{r}_1, \dots, \mathbf{r}_N)$ is the N -particle potential energy function. We will assume there exists a set of collective coordinates $q_1(\mathbf{r}), \dots, q_n(\mathbf{r})$, $n < N$, that characterize conformational changes in a system. We are interested in characterizing the multidimensional free-energy surface $F(q_1, \dots, q_n)$. Consider, therefore, introducing a change of variables in eq 1

$$\begin{aligned} q_1 &= q_1(\mathbf{r}_1, \dots, \mathbf{r}_N) \\ q_2 &= q_2(\mathbf{r}_1, \dots, \mathbf{r}_N) \\ &\dots \\ q_{3N} &= q_{3N}(\mathbf{r}_1, \dots, \mathbf{r}_N) \end{aligned} \quad (2)$$

where the first n of these coordinates are of primary interest. Introducing the coordinate transformation into eq 1 gives

$$Q(N,V,T) = \frac{1}{N!h^{3N}} \int d^N \mathbf{p} \int_{D(V)} d^{3N} q J(q) \times \exp \left\{ -\beta \left[\sum_{i=1}^N \frac{\mathbf{p}_i^2}{2m_i} + U(\mathbf{r}_1(q), \dots, \mathbf{r}_N(q)) \right] \right\} \quad (3)$$

where $q = q_1, \dots, q_{3N}$ denotes the complete set of coordinates in eq 2, $J(q) = |\partial \mathbf{r} / \partial q|$ is the Jacobian of the transformation, and $\mathbf{r}_i(q)$ are the original Cartesian coordinates expressed as functions of the new coordinates, i.e., the inverse of eq 2. If the Jacobian is absorbed into the exponential and an effective potential

$$\tilde{U}(q_1, \dots, q_{3N}) = U(\mathbf{r}_1(q), \dots, \mathbf{r}_N(q)) - \frac{1}{\beta} J(q_1, \dots, q_{3N}) \quad (4)$$

is defined, then the transformed partition function

$$Q(N,V,T) = \frac{1}{N!h^{3N}} \int d^N \mathbf{p} \int_{D(V)} d^{3N} q \times \exp \left\{ -\beta \left[\sum_{i=1}^N \frac{\mathbf{p}_i^2}{2m_i} + \tilde{U}(q_1, \dots, q_{3N}) \right] \right\} \quad (5)$$

is of the same form as eq 1 and can be generated via thermostated MD using as a Hamiltonian

$$H = \sum_{i=1}^N \frac{\mathbf{p}_i^2}{2m_i} + \tilde{U}(q_1, \dots, q_{3N}) \quad (6)$$

In eq 6, the original Cartesian momenta are treated as if they were "conjugate" to the new coordinates. Consequently, eq 6 cannot be used to generate the dynamics of the system. However, as was shown in refs 16 and 19, eq 6 is the starting point for the development of powerful enhanced conformational sampling techniques. In the AFED method, an adiabatic separation is achieved between the first n coordinates and the remaining degrees of freedom by adjusting their characteristic frequencies so as to make them considerably lower than all other frequencies in the system. This condition can be realized by choosing a set of masses $\tilde{m}_1, \dots, \tilde{m}_n$ for the first n coordinates that are larger than the remaining $3N - n$ masses.³³ This gives an effective AFED Hamiltonian of the form

$$H = \sum_{\alpha=1}^n \frac{p_{\alpha}^2}{2\tilde{m}_{\alpha}} + \sum_{\alpha=n+1}^{3N} \frac{p_{\alpha}^2}{2m_{\alpha}} + \tilde{U}(q_1, \dots, q_{3N}) \quad (7)$$

Note that the coordinates q_1, \dots, q_n do not need to be adiabatically decoupled from the remaining degrees of freedom in the true physical dynamics of the system. The adiabatic separation employed here is a fictitious one introduced (or imposed) as a means of enhancing the sampling along these first n coordinates and, thereby, generating the free-energy surface in an efficient manner.

In addition to the adiabatic separation, we assume that what makes the free-energy surface $F(q_1, \dots, q_n)$ interesting is its roughness. However, because a rough surface will be characterized by high barriers, it is necessary to enhance the barrier crossing frequency of the n reactive coordinates. This is achieved by introducing a temperature $T_q \gg T$ for these coordinates that is high enough to ensure that these barriers can be frequently crossed, allowing a statistically meaningful sampling of all

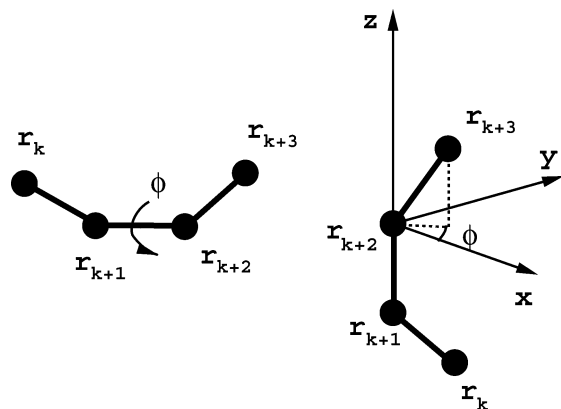


Figure 1. Illustration of the transformation used to resolve the backbone dihedral angles in an unbranched chain molecule.

basins and saddle points on the free-energy surface to be achieved. In MD, separate temperatures can be imposed by coupling the first n coordinates to thermostats at temperature T_q and the remaining coordinates to thermostats at temperature T .

A detailed analysis of the adiabatic dynamics with two separate temperatures was carried out in ref 16 employing the Liouville operator formalism. It was shown there that the dynamics samples a distribution of the n slow coordinates given by

$$P_{\text{adb}}(q_1, \dots, q_n) \propto \left\{ \int d q_{n+1} \dots d q_{3N} d^{3N} p \exp[-\beta(K(p) + \tilde{U}(q_1, \dots, q_{3N}))] \right\}^{\beta_q/\beta} \propto [\hat{Q}(q_1, \dots, q_n)]^{\beta_q/\beta} \quad (8)$$

where $\beta_q = 1/k_B T_q$, $K(p) = \sum_{\alpha=1}^n p_{\alpha}^2 / 2\tilde{m}_{\alpha} + \sum_{\alpha=n+1}^{3N} p_{\alpha}^2 / 2m_{\alpha}$, and $\hat{Q}(q_1, \dots, q_n)$ is a reduced partition function obtained by integrating $\exp(-\beta H)$ over all phase space variables except q_1, \dots, q_n . By definition, the free-energy surface $F(q_1, \dots, q_n)$ is given by

$$F(q_1, \dots, q_n) = -\frac{1}{\beta} \ln \hat{Q}(q_1, \dots, q_n) \quad (9)$$

From eq 8, it is clear that $F(q_1, \dots, q_n)$ can be obtained directly from the adiabatic probability distribution function $P_{\text{adb}}(q_1, \dots, q_n)$ via the formula

$$F(q_1, \dots, q_n) = -\frac{1}{\beta_q} \ln P_{\text{adb}}(q_1, \dots, q_n) + \text{constant} \quad (10)$$

Equation 10 shows that the free energy can be generated directly from the adiabatic probability distribution function without any unbiasing or *a posteriori* processing of the output data. Note that it is not necessary to know *a priori* exactly which is the optimal set of coordinates q_1, \dots, q_n for characterizing the free-energy surface. A reasonable guess is sufficient, because uninteresting or irrelevant coordinates can be integrated out subsequently to produce the reduced free-energy surface of particular interest.

In order to apply eq 10 to the backbone dihedral angles in a peptide chain, it is necessary to transform to a set of coordinates that contains these dihedral angles as explicit coordinates. Figure 1 shows how this can be accomplished. Consider the four atoms with Cartesian coordinates r_k , r_{k+1} , r_{k+2} , and r_{k+3} . We first transform to a coordinate system in which r_{k+3} is at the origin and the vector $r_{k+3} - r_{k+2}$ lies along the z axis. In this frame, the vector $r_{k+4} - r_{k+3}$ can be resolved into spherical polar coordinates $(r, \vartheta, \text{and } \varphi)$ and the azimuthal angle, φ , is equal

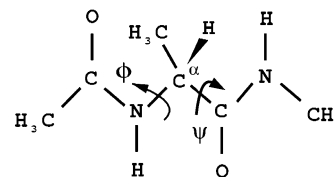


Figure 2. Schematic of the alanine dipeptide showing the ϕ and ψ angles.

to the dihedral angle. This transformation can be performed for each dihedral angle in succession (excluding the dihedral angles around the peptide bond), leading to a set of generalized coordinates that contain the Ramachandran (ϕ , ψ) angles as explicit coordinates.

In the present study, the following simulation protocol was employed. The initial configurations were obtained by equilibrating the systems for an average of 1 ns at a system temperature of $T = 300$ K in a cubic box with dimension $L = 25.64$ Å for the alanine dipeptide and $L = 26.00$ Å for the alanine tripeptide. Production AFED runs were then performed assigning a high temperature and mass to ϕ and ψ backbone dihedral angles for up to 10 ns simulation time. The NVT distribution was generated by coupling a Generalized Gaussian Moment Thermostat (GGMT) of Liu and Tuckerman,³⁴ which was shown to be effective for adiabatic problems, to each degree of freedom in the system at its appropriate temperature.¹⁶ The equations of motion were integrated using the multiple time scale algorithm, RESPA³⁵ to exploit the separation in time scales between the intra- and intermolecular interactions. The use of RESPA allowed the use of an increased time step of 2 fs. All calculations were performed with the PINY_MD code.³⁹

3. Results and Discussion: Alanine Dipeptide

The alanine dipeptide is shown in Figure 2. The (ϕ, ψ) angles around the central C_{α} are shown in the figure. In applying the AFED method, these angles are treated as slow variables with mass $m_{(\phi, \psi)} = 50m_C$, where m_C is the mass of a carbon atom, heated to a temperature $T_{(\phi, \psi)} = 1500$ K. The dihedral angle ω around the peptide bond is not treated as an adiabatic variable. Parts a and c of Figure 3 show the two-dimensional free-energy surface $F(\phi, \psi)$ and Ramachandran contour map, respectively, generated with the AFED method for the alanine dipeptide in the gas phase. Also shown in Figure 3a is the same surface generated using the two-dimensional umbrella sampling combined with the weighted histogram (WHAM) approach.³⁶ The figure shows that the AFED and umbrella sampling approaches agree well with each other, which serves to benchmark the AFED method against a widely used and well-tested approach. AFED is able to generate the two-dimensional profiles using simulation lengths of 3.5 ns out of the total 10 ns simulated, compared to 35.2 ns for umbrella sampling using a force constant of 20 000 K/rad² and 176 windows. Thus, the real power of the AFED method becomes clear; multidimensional surfaces can be generated with a substantial increase in computational efficiency compared to a method such as umbrella sampling, which requires a full two-dimensional grid of simulations. The structure of the gas-phase free-energy surface in Figure 3a is in agreement with other simulation studies on the alanine dipeptide employing the CHARMM22 force field.³⁷ In particular, we obtain a minimum at $(\phi, \psi) = (-81, 81)$, corresponding to an extended β structure. A second minimum occurs at $(\phi, \psi) = (63, -81)$ approximately 2.3 kcal/mol above the β minimum, corresponding to a C_7^{ax} extended conformation.

Solution-phase calculations were performed by solvating the alanine dipeptide in a bath of 558 water molecules in a 25.64

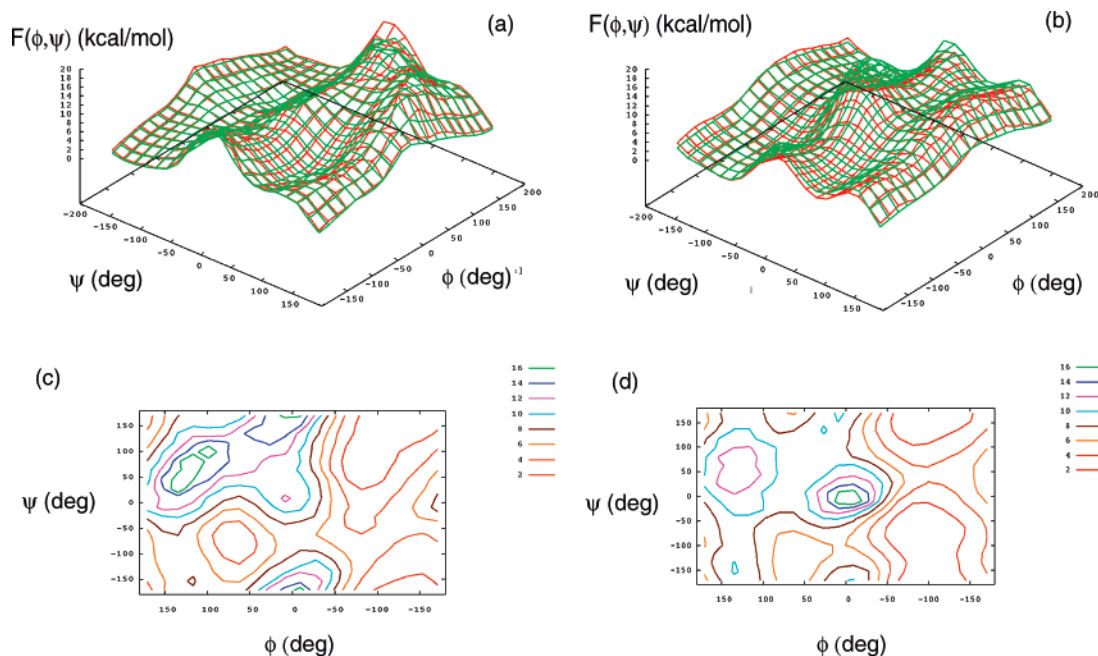


Figure 3. (a) Free-energy surface $F(\phi, \psi)$ for the alanine dipeptide in the gas phase generated using AFED (red) and umbrella sampling (green). (b) Same as for a except in solution. (c) Ramachandran contour map corresponding to the free-energy surface in a for the alanine dipeptide in the gas phase. (d) Same as in c except corresponding to free-energy surface in b, i.e., solvated alanine dipeptide.

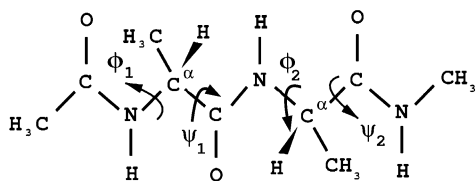


Figure 4. Schematic of the alanine tripeptide showing the two sets of ϕ and ψ angles.

Å periodic box. Electrostatics were treated using the smooth particle mesh Ewald summation technique,⁴⁰ while short-range forces were switched off at a distance of 10 Å. Run lengths of 35.2 ns and 4.7 ns were used for umbrella sampling and AFED, respectively. Shorter run lengths with umbrella sampling were found to give rise to “holes” in the distribution due to inadequate sampling. Parts b and d of Figure 3 show the two-dimensional free-energy surface in solution for AFED and umbrella sampling and corresponding Ramachandran contour map, respectively. Parts c and d of Figure 3 show that AFED is able to generate a complete free-energy surface and Ramachandran contour map that agrees with umbrella sampling; however, it can achieve this almost 7.5 times more efficiently than umbrella sampling using the same parameters as in the gas phase for both methods. Both figures show that, in solution, a new minimum appears at $(\phi, \psi) = (-81, -63)$ corresponding to a right-handed α -helical conformation, while the β conformation now occurs at $(\phi, \psi) = (-81, 153)$ at an energy of 0.2 kcal/mol above the α -helical minimum. The extended C_7^{ax} conformation occurs as a local minimum as well at $(\phi, \psi) = (63, -117)$ but has an energy of 4.5 kcal/mol above the minimum. These values are in very good agreement with previous simulation results^{24,38} using the same force field and a biasing potential for a 100 ns simulation.

4. Results and Discussion: Alanine Tripeptide

In comparison to the alanine dipeptide, which has been extensively studied, the alanine tripeptide has received considerably less attention in the literature. Figure 4 shows a schematic of the alanine tripeptide with its two sets of ϕ and ψ angles.

The figure makes clear that the alanine tripeptide is not equivalent to trialanine, which has been studied recently both experimentally⁷ and theoretically.^{25,29–32} MD simulations with biasing potentials²⁹ show that the alanine tripeptide fills the same regions of the Ramachandran plot as the alanine dipeptide. It is important to note that the free-energy surfaces for each dihedral angle pair (ϕ_1, ψ_1) and (ϕ_2, ψ_2) are very similar. Figure 4a shows the free-energy surface for one such pair obtained with the AFED method with mass $m_{(\phi, \psi)} = 50m_C$ and temperature $T_{(\phi, \psi)} = 1500$ K. Examination of the free-energy surfaces depicted in Figure 4a and the contour plots in Figure 4b for the alanine tripeptide in the gas phase show the C_7^{ax} , which occurs at $(\phi_2, \psi_2) = (63, -81)$ at an energy of approximately 2.2 kcal/mol above the minimum and has a more pronounced basin than in the alanine dipeptide. The minimum occurs at $(\phi_2, \psi_2) = (-81, 81)$, corresponding to an extended β conformation. Solution-phase calculations were performed by solvating the alanine tripeptide in a bath of 558 water molecules in a 26.00 Å periodic box, with the same treatment of electrostatics and short-range forces as in the previous section. The AFED technique was applied imposing a mass $m_{(\phi, \psi)} = 50m_C$ and a temperature $T_{(\phi, \psi)} = 1500$ K. In solution, the global minimum becomes the right-handed α -helical conformation, and the C_7^{ax} conformation is destabilized by approximately an additional 2.6 kcal/mol. Once again, the α -helix and β conformations have approximately the same free energy for this force field.

For the alanine tripeptide, a comparison between AFED and umbrella sampling is made only for the alanine tripeptide in the gas phase (see Figure 4a), where it is found that good agreement is obtained. AFED simulations are able to reproduce the free-energy surface using only 4.7 ns of the 10 ns simulated, while umbrella sampling requires 50 ns of simulation time when a force constant of 20 000 K/rad² was used with 169 sampling windows in conjunction with WHAM. For these parameters, AFED is roughly 10 times more efficient than umbrella sampling. As with the alanine dipeptide, it was found that shorter umbrella sampling runs led to “holes” in the distribution as a result of inadequate sampling. Having shown that AFED is able

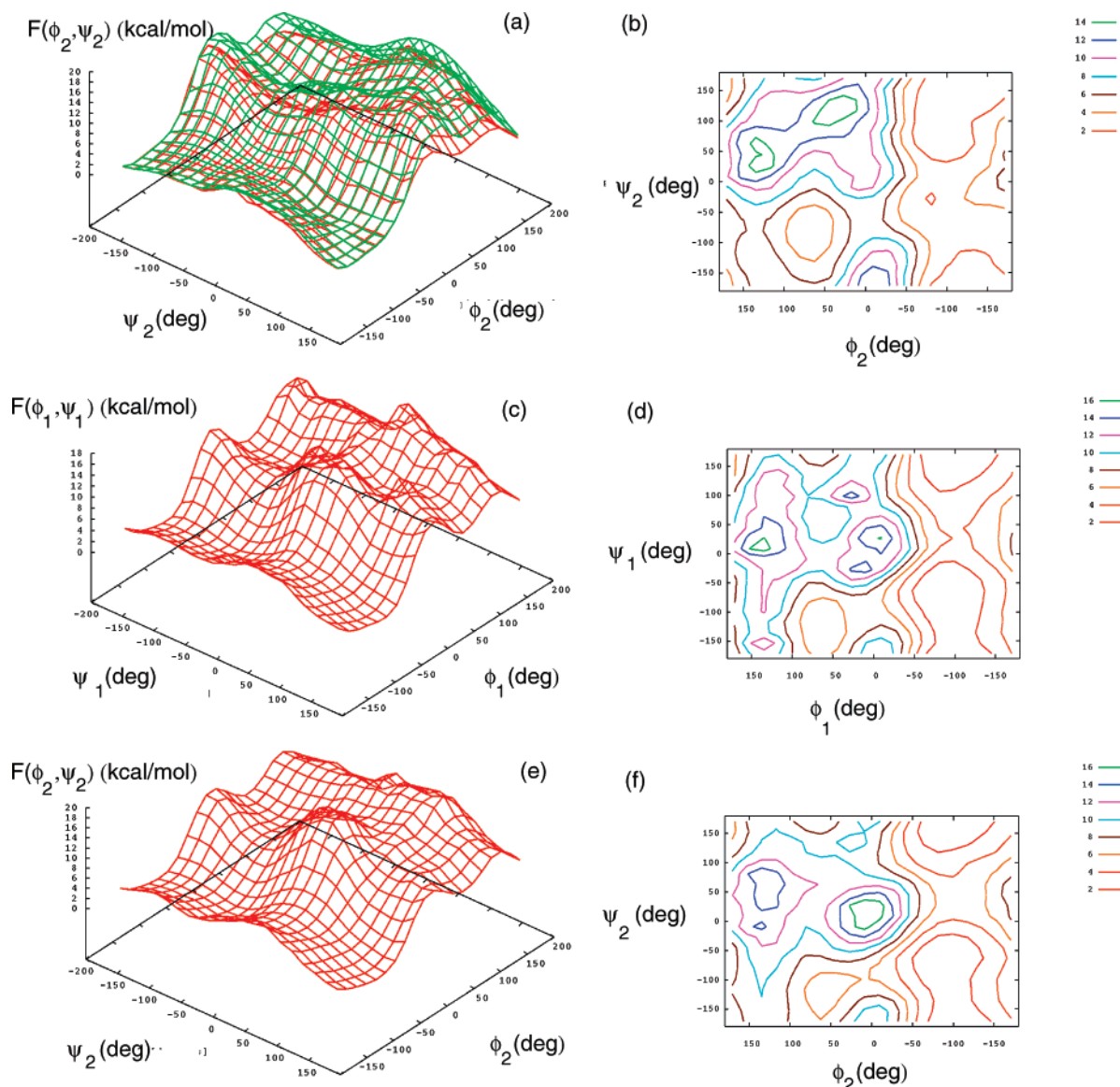


Figure 5. (a) Free-energy surface $F(\phi_2, \psi_2)$ for the alanine tripeptide in the gas phase generated using AFED (red) and umbrella sampling (green). (b) Corresponding Ramachandran contour map. (c) Free-energy surface $F(\phi_1, \psi_1)$ corresponding to the alanine tripeptide in solution generated using AFED. (d) Corresponding Ramachandran contour map. (e) Same as in c except for the (ϕ_2, ψ_2) pair. (f) Same as in d except for the (ϕ_2, ψ_2) pair.

to reproduce the same surface as umbrella sampling, we employed it to predict the free-energy surface in solution. The surfaces shown in parts c and e of Figure 4 were generated using the simulation of length at approximately 5 ns. Corresponding Ramachandran contour maps are shown in parts d and f of Figure 4. The figure shows the surfaces obtained for both pairs of dihedral angles to show that sufficient sampling is obtained to yield very similar surfaces. As with the alanine dipeptide, it is found that, in solution, a free-energy minimum corresponding to the right-handed α -helical structure appears $(\phi_i, \psi_i) = (-81, -63)$, $i = 1, 2$, for both surfaces in addition to the extended β structure at $(\phi_i, \psi_i) = (-99, 171)$. As with the alanine dipeptide, these two structures are nearly isoenergetic with an energy difference of just 0.10 kcal/mol. Finally, the C_7^{ax} conformation occurs at $(\phi_i, \psi_i) = (63, -117)$ and at an energy of 4.87 kcal/mol above the global minimum.

5. Conclusion

AFED has been used to generate the Ramachandran free-energy surfaces of the alanine di- and tripeptides in a vacuum and in solution using the CHARMM22 force field. Direct

comparison to two-dimensional umbrella sampling has been made, and it has been found that AFED is able to generate the surfaces at a factor of at least 7 more efficiently than the latter. For the alanine dipeptide, the structure of the free-energy surface is found to be in good agreement with previous simulations using the same force field.^{24,38} Because much less is known about the alanine tripeptide, the present calculations can be viewed as a detailed exploration of this surface. It has been shown that, while the β and right-handed α -helix quadrants of the Ramachandran map are similar to the alanine dipeptide, the C_7^{ax} conformation appears to have a deeper basin for the alanine tripeptide in a vacuum for the present force field. This conformation is destabilized by approximately 2–3 kcal/mol in solution, where the right-handed α helix is the lowest free-energy state. The present calculations show that the AFED approach is a potentially powerful tool for studying multi-dimensional free-energy surfaces (Figure 5).

Acknowledgment. This work was supported by NSF CHE-0310107, an NYU Research Challenge fund grant and the Camille and Henry Dreyfus Teacher–Scholar Award program.

References and Notes

- (1) Creighton, T. E. *Proteins: Structure and Molecular Properties*; W. H. Freeman and Company: New York, 1984.
- (2) Marqusee, S.; Robbins, V. H.; Baldwin, R. L. *Proc. Natl. Acad. Sci. U.S.A.* **1989**, *86*.
- (3) Miick, S. M.; Martinez, G. V.; Fiori, W. R.; Todd, A. P.; Millhauser, G. L. *Nature* **1992**, *359*.
- (4) Lee, D. K.; Ramamoorthy, A. *J. Phys. Chem. B* **1999**, *103*.
- (5) Woutersen, S.; Mu, Y.; Stock, G.; Hamm, P. *Proc. Natl. Acad. Sci. U.S.A.* **2001**, *98*.
- (6) Dian, B. C.; Longarte, A.; Zwier, T. S. *Science* **2002**, *296*.
- (7) Shi, Z. S.; Olson, C. A.; Rose, G. D.; Baldwin, R. L.; Kallenbach, N. R. *Proc. Natl. Acad. Sci. U.S.A.* **2002**, *99*.
- (8) Berg, B. A.; Neuhaus, T. *Phys. Rev. Lett.* **1992**, *68*, 9.
- (9) Marinari, E.; Parisi, G. *Europhys. Lett.* **1992**, *19*, 451.
- (10) Hansmann, U. H. E. *Physica A* **1997**, *242*, 250.
- (11) Hansmann, U. H. E.; Okamoto, Y. *Phys. Rev. E* **1997**, *56*, 2228.
- (12) Sugita, Y.; Kitao, A.; Okamoto, Y. *J. Chem. Phys.* **2000**, *113*, 6042.
- (13) Bartels, C.; Karplus, M. *J. Comput. Chem.* **1997**, *18*, 1450.
- (14) Samuelson, S.; Tobias, D. J.; Martyna, G. J. *J. Phys. Chem. B* **1997**, *101*, 7592.
- (15) Laio, A.; Parrinello, M. *Proc. Natl. Acad. Sci. U.S.A.* **2002**, *99*, 12562.
- (16) Rosso, L.; Minari, P.; Zhu, Z.; Tuckerman, M. E. *J. Chem. Phys.* **2002**, *116*, 4389.
- (17) Zhu, Z.; Tuckerman, M. E.; Samuelson, S. O.; Martyna, G. J. *Phys. Rev. Lett.* **2002**, *88*, 100201.
- (18) VandeVondele, J.; Rothlisberger, U. *J. Phys. Chem. B* **2002**, *106*, 203.
- (19) Rosso, L.; Tuckerman, M. E. *Mol. Simul.* **2002**, *28*, 925.
- (20) Torrie, G. M.; Valleau, J. J. *J. Comput. Phys.* **1977**, *23*, 187.
- (21) Carter, E. A.; Ciccotti, G. *Chem. Phys. Lett.* **1989**, *156*, 472.
- (22) Sprik, M.; Ciccotti, G. *J. Chem. Phys.* **1998**, *109*, 7737.
- (23) Roterman, I. K.; Lamberg, M. H.; Gibson, K. D.; Scheraga, H. A. *J. Mol. Biol. Struct. Dyn.* **1989**, *7*, 421.
- (24) Tobias, D. J.; Brooks, C. L. *J. Phys. Chem.* **1992**, *96*, 3864.
- (25) Samuelson, S.; Hughes, A.; Martyna, G. J. *J. Chim. Phys.* **1997**, *94*, 1503.
- (26) Vargas, R.; Garza, J.; Hay, B. P.; Dixon, D. A. *J. Phys. Chem. A* **2002**, *106*, 3213.
- (27) Hu, H.; Elstner, M.; Hermans, J. *Proteins: Struct., Funct., Genet.* **2003**, *50*, 451.
- (28) Feig, M.; MacKerell, A. D.; Brooks, C. L. *J. Phys. Chem. B* **2003**, *107*, 2831.
- (29) Straatsma, T. P.; McCammon, J. A. *J. Chem. Phys.* **1994**, *101*.
- (30) Beglov, D.; Roux, B. *Biopolymers* **1995**, *35*.
- (31) Mirkin, N. G.; Krimm, S. *J. Phys. Chem. A* **2002**, *106*.
- (32) Fukuda, I.; Nakamura, H. *J. Phys. Chem. B* **2004**, *108*.
- (33) Bennett, C. H. *J. Comput. Phys.* **1975**, *19*, 267.
- (34) Liu, Y.; Tuckerman, M. E. *J. Chem. Phys.* **2000**, *112*, 1685.
- (35) Tuckerman, M. E.; Martyna, G. J.; Berne, B. J. *J. Chem. Phys.* **1992**, *97*, 1990.
- (36) Ferrenberg, A. M.; Swendsen, R. H. *Phys. Rev. Lett.* **1989**, *63*, 1195.
- (37) MacKerell, A., Jr.; Bashford, D.; Bellott, M.; Dumbrack, R. L.; Evanseck, J. D.; Field, M. J.; Fischer, S.; Guo, H.; Ha, S.; Joseph-McCarthy, D.; Kucznir, L.; Kuczera, K.; Lau, F.; Mattos, C.; Michnick, S.; Ngo, T.; Nguyen, D. T.; Prodhom, B.; Reiher, W. E., III; Roux, B.; Schlenkrich, M.; Smith, J. C.; Stote, R.; Straub, J.; Watanabe, M.; Wiorkiewicz-Kuczera, J.; Yin, D.; Karplus, M. *J. Phys. Chem. B* **1998**, *102*, 3586.
- (38) Smith, P. E. *J. Chem. Phys.* **1999**, *111*, 5568.
- (39) Tuckerman, M. E.; Yarne, D. A.; Samuelson, S. O.; Hughes, A. L.; Martyna, G. J. *Comp. Phys. Comm.* **2000**, *128*, 333.
- (40) Essmann, U.; Perera, L.; Berkowitz, M. L.; Darden, T.; Lee, H.; Pedersen, L. G. *J. Chem. Phys.* **1995**, *103*, 8577.